The influence of degree of saturation on the coefficient of aqueous diffusion

P.C. Lim, S.L. Barbour, and D.G. Fredlund

Abstract: The role of degree of saturation on the coefficient of diffusion of contaminants in the aqueous phase is presented and theoretical models for predicting the coefficient of diffusion at any degree of saturation are described. Three predictive models were developed based on three different diffusion modes: diffusion in parallel and series arrangements and combination of both. Diffusion tests were conducted on a sand at various water contents ranging from saturation to the residual degree of saturation using potassium and chloride ions as tracers to verify the applicability of the models. Results from the diffusion tests showed a decrease in effective diffusion coefficient of potassium with a decrease in degree of saturation. The functional relationship between the normalized diffusion coefficient for potassium and the degree of saturation is slightly nonlinear. The results for chloride also showed a decreasing trend, although the data were quite scattered and further verification is needed. Model verification based on the results for potassium showed that among the three models proposed, the model which combines the diffusion pathways in parallel and series arrangements provides the best fit to the experimental data.

Key words: unsaturated, contaminant transport, aqueous diffusion, degree of saturation.

Résumé : L'on présente le rôle du degré de saturation sur le coefficient de diffusion de contaminants dans la phase aqueuse, et l'on décrit des modèles théoriques pour prédire le coefficient de diffusion à n'importe quel degré de saturation. Trois modèles de prédiction ont été développés sur la base de trois modes différents de diffusion: diffusion dans des arrangements en parallèle et en série, et dans une combinaison des deux. Les essais de diffusion ont été réalisés sur un sable à différentes teneurs en eau, s'étendant de la saturation au degré de saturation résiduel utilisant du potassium et des ions de chlorure comme traceur pour vérifier l'applicabilité des modèles. Les résultats d'essais de diffusion ont montré une diminution dans le coefficient effectif de diffusion du potassium avec une diminution du degré de saturation. La relation de la fonction entre le coefficient de diffusion normalisé pour le potassium et le degré de saturation est légèrement non linéaire. Les résultats pour le chlorure ont également montré une tendance à la diminution quoique les données étaient dispersées; une vérification supplémentaire est requise. La vérification du modèle basée sur les résultats pour le potassium a montré que parmi les trois modèles proposés, le modèle qui combine les cheminements dans les arrangements en parallèle et en série fournit la meilleure concordance avec les résultats expérimentaux.

Mots clés : non saturé, transport de contaminant, diffusion aqueuse, degré de saturation.

[Traduit par la Rédaction]

Introduction

Aqueous diffusion is often the dominant mechanism governing the movement of dissolved contaminants when the hydraulic gradient or the hydraulic conductivity of subsurface materials is low. In some applications such as the use of engineered clay soil as liner material, it may be desirable to control the rates of contaminant diffusion away from hazardous waste sites. One possible method of controlling diffusion is to reduce the coefficient of diffusion or to eliminate the pathways available for diffusion. For example, Allison and Bergmen (1988) and Conca and Wright (1990) used unsaturated gravel as a moisture and diffusion barrier.

Received September 17, 1997. Accepted June 18, 1998.

P.C. Lim. CL-GEO Consultants, 144 Thomson Green, Singapore 574998.
S.L. Barbour and D.G. Fredlund. Department of Civil Engineering, University of Saskatchewan, Saskatoon, SK S7N 5A9, Canada.

This paper addresses the role of degree of saturation on the effective diffusion coefficient of solute within the aqueous phase in soil. The dependency of the coefficient of diffusion on soil water content for different textured soils has been reported by previous researchers (Klute and Letey 1958; Porter et al. 1960; Romkens and Bruce 1964; Rowell et al. 1967; Warncke and Barber 1972; Barraclough and Tinker 1981; Conca and Wright 1990). The form of the functional relationship between the effective diffusion coefficient and water content also varies with soil type. For a given soil, a comprehensive testing program is often required to determine the effective diffusion coefficient at different stress states (i.e., different density and matric-suction conditions). Diffusion testing of unsaturated soil is, therefore, very time consuming and costly.

An empirical relationship between the effective diffusion coefficient, normalized with respect to the diffusion in free water, and the volumetric water content has been proposed by Olsen and Kemper (1968). Numerous tests, however, are still required to define the empirical constant(s). The objectives of this paper are to develop theoretical models for pre-

dicting the coefficient of diffusion and to verify the application of the models. Diffusion tests were conducted on sand at various suctions to characterize the effective diffusion coefficients of chloride and potassium as a function of degrees of saturation.

Background

Aqueous diffusion is a process whereby dissolved mass is transported from a higher potential towards a lower potential by random molecular motion (Robinson and Stokes 1959). Diffusion in free water can be described mathematically by Fick's law. A detailed treatment of the fundamental basis of Fick's first law for steady-state diffusion has been presented by Shackleford and Daniel (1991). The driving energy responsible for the diffusion of ions, atoms, or molecules is attributed to a change in chemical potential, or concentration for dilute solution.

The mechanism governing the diffusion of ions in free water is also operative in soil water. The diffusive mass flux in soil is, however, smaller than the flux in free water. The reduction in diffusive flux is attributed to two factors: first, the open area available for diffusion is reduced; and second, the diffusion pathways are more tortuous in soil. The one-dimensional steady-state diffusive flux of ion i in soil can be written as

$$[1] \qquad J_m = -\theta_w D_i^* \frac{dC_i}{dz}$$

where

J_m is the mass flux;
dC_i is the change in concentration of ion i in soil water over an elemental volume;
dz is the macroscopic distance of an elemental volume;
θ_w is the volumetric water content of the soil; and
D_i^* is the effective diffusion coefficient of ion i in soil.

For a saturated soil, the effective diffusion coefficient under a given state of stress is a constant, and is defined by Porter et al. (1960) as

$$[2] \qquad D_i^* = D_i^o (L/L_e)^2 \gamma$$

where

D_i^o is the diffusion coefficient of ion i in free water;
$(L/L_e)^2$ is a geometric factor which accounts for the effect of tortuous pathways;
L is the macroscopic distance across an elemental soil volume;
L_e is the length of actual diffusion pathway across the elemental soil volume; and
γ is a factor which includes both the effects of ionic interaction and the increased viscosity of water in the immediate vicinity of a soil particle.

For an unsaturated soil, the effective diffusion coefficient given in eq. [2] is no longer a constant but varies with water content:

$$[3] \qquad D_i^*(\theta_w) = D_i^o (L/L_e)^2 \gamma$$

Equation [3] can also written as a function of the degree of saturation S:

$$[4] \qquad D_i^*(S) = f(S) D_i^o$$

where f is a tortuosity factor which includes both the geometric factor and the ionic interaction and viscosity effects.

Studies have shown that the effective diffusion coefficient decreases with decreases in the water content of the soil (Porter et al. 1960; Romkens and Bruce 1964; Rowell et al. 1967; Warncke and Barber 1972; Barraclough and Tinker 1981) (Fig. 1; Table 1). The functional relationships between the coefficient of diffusion and water content for glass beads, sandy soils, and gravel are nonlinear. However, the functional relationships for fine-grained soils such as loam, sandy loam, silty loam, and clay were shown to be either linear or slightly nonlinear.

Most researchers have attributed the decrease in the effective diffusion coefficient with a decrease in water content to an increase in the diffusion path length. Other factors that may have an important influence on the effective diffusion coefficient include increased viscosity of liquid next to the soil particle, increased ionic interaction along small pores and water films, and interconnectivity between the water-filled pores and the water films (Porter et al. 1960; Romkens and Bruce 1964; Rowell et al. 1967; Warncke and Barber 1972; Barraclough and Tinker 1981).

The only empirical relation describing the dependency of the effective diffusion coefficient on the volumetric water content was that proposed by Olsen and Kemper (1968):

$$[5] \qquad D_i^*(S) = D_i^o K e^{b\theta_w}$$

where K and b are empirical constants. Equation [5] is said to be applicable only for suctions between 33 and 1500 kPa. Van Rees (1989) applied the empirical relation to the results of Porter et al. (1960), Rowell et al. (1967), Warncke and Barber (1972), and Barraclough and Tinker (1981) for loamy soils and obtained a value of 3.13 and 1.92 for K and b, respectively.

The effect of degree of saturation on the effective coefficient holds true for both nonreactive and reactive contaminants. However, for reactive contaminant, the contaminant can be further removed from the soil water by adsorption. The adsorption characteristic of a soil can be described by Freundlich's equation:

$$[6] \qquad Q_{ad} = K_f(S)(C_f)^m$$

where

Q_{ad} is the mass adsorbed by the soil per unit mass of dry soil;
$K_f(S)$ is the adsorption coefficient as a function of the degree of saturation;
C_f is the equilibirum or final concentration; and
m is the shape factor.

Theory

The development of a model for predicting the functional relation for the coefficient of diffusion at various degrees of saturation is described. The theoretical framework was conceptualized based on the role of water content on diffusion at various suctions. The key considerations are the distribution of the liquid phase, the nature of the various diffusion pathways, and the interconnectivity of the liquid phase.

The pore-water distribution at a microscopic level can be subdivided into the liquid phase distributed as water-filled

Fig. 1. Relationship between the effective diffusion coefficient, normalized with respect to the diffusion coefficient in free water, and the volumetric water content for various geologic materials.

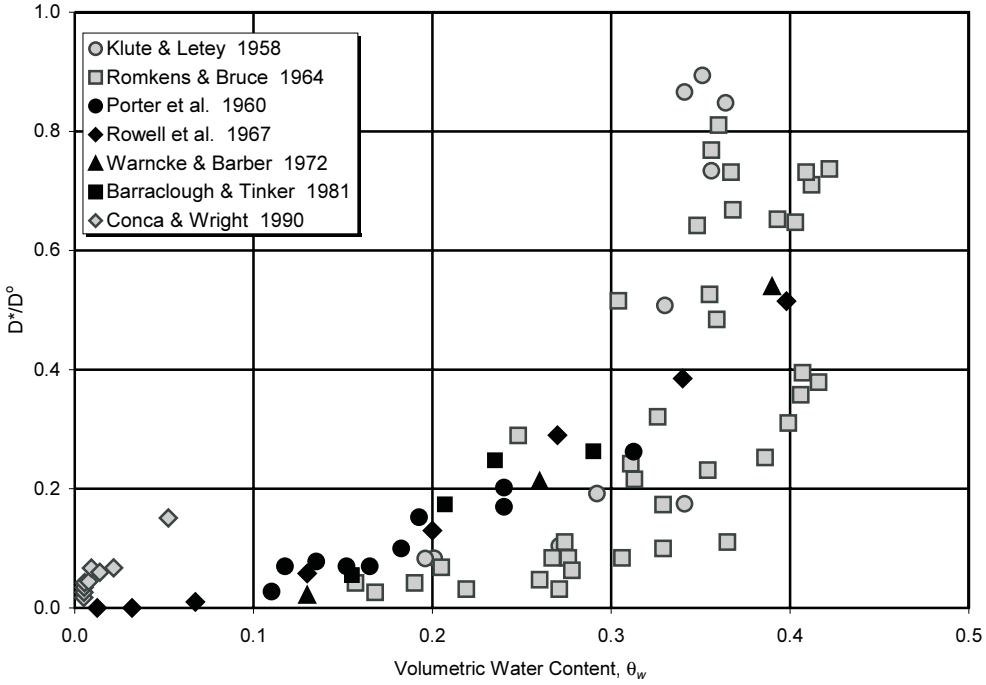

Table 1. Summary of the test methodology and the shape of the functional relationship for the effective diffusion coefficient reported by previous researchers.

Reference	Method of measurement	Material	Chemical species	Form of the functional relation
Klute and Letey 1958	Two half cells	Glass beads	^{86}Rb	Nonlinear
Porter et al. 1960	Two half cells	Loam, silty clay, and clay	Cl^-/ NO_3^-	Linear
Romkens and Bruce 1964	Two half cells	Glass beads and sand	NO_3^-	Nonlinear
Rowell et al. 1967	Two half cells	Sandy loam	^{36}Cl	Nonlinear
Warncke and Barber 1972	One half cell with exchange resin paper	Silty clay loam	^{36}Cl	Nonlinear
Barraclough and Tinker 1981	One half cell with exchange membrane	Sandy loam and silty clay loam	Cl^-	Bilinear
Conca and Wright 1990	Electrical conductivity method	Angular granitic gravel	0.1 M KCl	Nonlinear

pores, water films along the solid–air boundaries, and water in wedge-shaped volumes (i.e., water in the pore throats). The proportion of each component, however, varies as the water content decreases from 100% saturation to the residual degree of saturation. At high degrees of saturation, the liquid phase is present predominantly as water-filled pores, and the fraction of water films and water in wedge-shaped volumes is small by comparison. As the degree of saturation decreases, the proportion of water-filled pores decreases and, conversely, the fraction of the water held in water films increases. Near the residual degree of saturation, the liquid phase is distributed predominantly as water films and as water in wedge-shaped volumes interconnected with the water films or isolated.

The pathways for diffusion were idealized as comprising interconnected water-filled pores, water films, and isolated water pockets over the range of water content from 100% to the residual degree of saturation. Three diffusion modes were considered: case I, in which diffusion is assumed to occur independently along continuous water-filled pores and water films in a parallel arrangement; case II, in which diffusion is assumed to occur along interconnected water-filled pores and water films in a series arrangement; and case III, in which diffusion is assumed to occur in an arrangement combining those of cases I and II. The diffusion models for cases I and II are illustrated in Fig. 2. The models further assume that diffusion will occur as long as the various pathways are continuous.

Fig. 2. Schematic illustration of the different modes of diffusion for cases I and II.

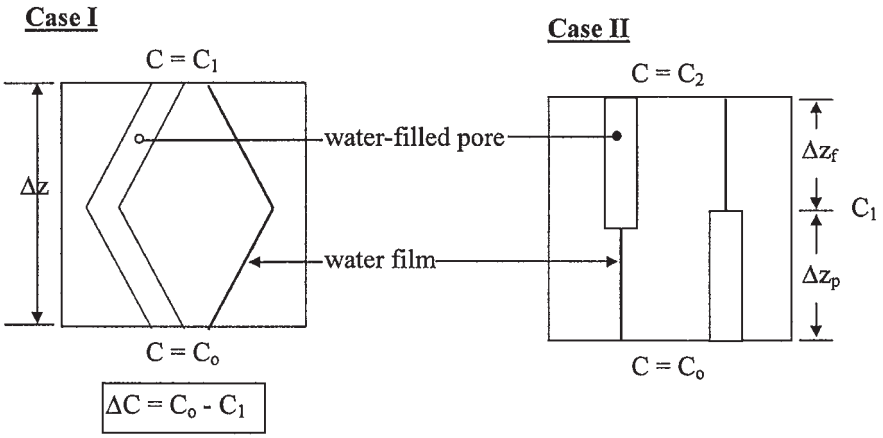

Case I

The mass flux for steady-state diffusion along independent water-filled pores and water films in a parallel arrangement can be written as follows:

$$[7] \qquad J_m = J_p + J_f$$

where

J_m is the macroscopic diffusive mass flux;
J_p is the diffusive mass flux along the water-filled pores; and
J_f is the diffusive mass flux along the water films.

Expanding the diffusive mass flux terms and setting the volumetric water content equal to the product of the porosity and the degree of saturation gives

$$[8] \qquad nSD^*(S)\frac{\Delta C}{\Delta z} = nS_pD^p(S)\frac{\Delta C}{\Delta z} + nS_fD^f(S)\frac{\Delta C}{\Delta z}$$

where

n is the porosity;
S is the degree of saturation or volume of water per volume of voids;
S_p is the volume of water-filled pores per volume of voids;
S_f is the volume of water films per volume of voids;
$D^*(S)$ is the macroscopic effective diffusion coefficient;
$D^p(S)$ is the effective diffusion coefficient along water-filled pores;
$D^f(S)$ is the effective diffusion coefficient along water films; and
$\Delta C/\Delta z$ is the macroscopic concentration gradient across the elemental volume (see Fig. 2).

Rearranging eq. [8] and expressing the effective diffusion coefficient in terms of the diffusion coefficient in free water gives

$$[9] \qquad D^*(S) = \frac{S_p}{S} f_p(S)D^o + \frac{S_f}{S} f_f(S)D^o$$

where

$f_p(S)$ is the tortuosity factor along the water-filled pores;
$f_f(S)$ is the tortuosity factor along the water films; and
D^o is the diffusion coefficient of ion in free water.

The terms S_p, S_f, $f_p(S)$, and $f_f(S)$ in eq. [9] are unknown. The tortuosity along the water-filled pores is also different from the tortuosity along the water films. To reflect the effect of degree of saturation on the effective diffusion coefficient, it is preferable to normalize the effective diffusion coefficient with respect to the effective diffusion coefficient at saturation:

$$[10] \qquad \frac{D^*(S)}{D^*(S=1)} = \frac{\frac{S_p}{S} f_p(S)D^o}{fD^o} + \frac{\frac{S_f}{S} f_f(S)D^o}{fD^o}$$

where $D^*(S = 1)$ is effective diffusion coefficient at S = 100%; and f is the tortuosity factor at S = 100%.

The distribution of the water between the water-filled pores and the water films at various degrees of saturation is unknown. The fraction of water contained in water films was assumed to increase linearly with a decreasing degree of saturation. At the residual degree of saturation, S_r, the fraction of water contained in water films, α, can be calculated based on the total surface area of the soil particles and an assumed water film thickness. The fraction of the water present as water films at any degree of saturation can be written as

$$[11] \qquad S_f = \alpha S_r \frac{(1-S)}{(1-S_r)}$$

or

$$[12] \qquad S_f = \alpha S_r(1-S_e)$$

where S_e is the effective saturation defined by Brooks and Corey (1966) as

$$[13] \qquad S_e = \frac{(S-S_r)}{(1-S_r)}$$

Correspondingly, the fraction of the water-filled pores at any given degree of saturation can be written as

$$[14] \qquad S_p = S - [\alpha S_r(1-S_e)]$$

Substituting eqs. [12] and [14] into eq. [10] gives

$$[15]\quad \frac{D^*(S)}{D^*(S=1)} = \frac{[S-\alpha S_r(1-S_e)]}{S}\frac{f_p(S)}{f} + \frac{\alpha S_r(1-S_e)}{S}\frac{f_f(S)}{f}$$

The increase in tortuosity in water-filled pores is assumed to vary proportionately, but inversely, with the degree of saturation. In the case of the water film, $[\alpha S_r(1 - S_e)/S]$ is small; however, regardless of how small the volume fraction, the water film remains a valid pathway as long as it is continuous. The contribution of the water film to diffusion is reflected by $(1 - S_e)$. The remaining terms $[\alpha S_r/S]$ and $f_f(S)/f$ can be combined to represent the increased resistance along the water film, $\Re$, which can be described by Renkin's (1955) model for diffusion along a small pore:

$$[16]\quad \Re = \left(1-\frac{\alpha}{\rho}\right)^2\left[1-2.1\left(\frac{\alpha}{\rho}\right)+2.09\left(\frac{\alpha}{\rho}\right)^3-0.95\left(\frac{\alpha}{\rho}\right)^5\right]$$

where

$\Re$ is a factor which includes both the entrance effect and the effects of increasing viscosity and ionic interaction along small pores; and

a/r is the ratio of the radius of the hydrated ion to the radius of the pore.

The effect of degree of saturation on the effective diffusion coefficient for case I is written as

$$[17]\quad \frac{D^*(S)}{D^*(S=1)} = \left(1-\frac{\alpha S_r(1-S_e)}{S}\right)S + (1-S_e)\Re$$

Case II

The mass flux for a steady-state diffusion along the interconnected water-filled pores and water films in a series arrangement is given as

$$[18]\quad J_m = J_p = J_f$$

The macroscopic diffusive mass flux across the elemental volume is given as

$$[19]\quad J_m = -nSf(S)D^o\frac{(C_o - C_2)}{\Delta z}$$

where

C_o is the concentration at the base of the elemental volume;

C_2 is the concentration at the top of the elemental volume; and

Δz is the macroscopic length of the elemental volume.

The diffusive flux across the water-filled pores and the water films can be written as follows:

$$[20]\quad J_p = -nS_p f_p(S)D^o\frac{(C_o - C_1)}{\Delta z_p}$$

and

$$[21]\quad J_f = -nS_f f_f(S)D^o\frac{(C_1 - C_2)}{\Delta z_f}$$

where

C_1 is the concentration at the junction of the water-filled pores and the water films;

Δz_p is the macroscopic length of the water-filled pore; and

Δz_f is the macroscopic length of the water film.

The change in concentration across the elemental length, Δz, can also be written as

$$[22]\quad (C_o - C_2) = (C_o - C_1) + (C_1 - C_2)$$

Rearranging and substituting eqs. [19], [20], and [21] into eq. [22] gives

$$[23]\quad \frac{\Delta z}{SD^*(S)} = \frac{\Delta z_p}{S_p D^p(S)} + \frac{\Delta z_f}{S_f D^f(S)}$$

Rearranging eq. [23] and normalizing the effective diffusion coefficient with respect to the effective diffusion coefficient at 100% saturation gives

$$[24]\quad \frac{D^*(S)}{D^*(S=1)} = \frac{\Delta z}{\frac{S}{[S-\alpha S_r(1-S_e)]}\frac{\Delta z_p}{f_p(S)/f} + \frac{S}{[\alpha S_r(1-S_e)]}\frac{\Delta z_f}{f_f(S)/f}}$$

The inverse of those terms in the denominator in eq. [24] is similar to the respective terms in eq. [15]. Hence, eq. [24] can be written as

$$[25]\quad \frac{D^*(S)}{D^*(S=1)} = \frac{\Delta z}{\frac{\Delta z_p}{[1-\alpha S_r(1-S_e)/S]S} + \frac{\Delta z_f}{(1-S_e)\Re}}$$

For a unit elemental volume, the length of the diffusion pathway, Δz, is equal to one. The length of a water-filled pore, Δz_p, which is unknown, can be inferred from the soil-water characteristic curve. Based on capillary theory and assuming that the number of continuous pores is inversely proportional to the square of the pore radius (Hillel 1980), the fraction of water-filled pores at any degree of saturation is equal to S. The fraction of water films associated with the unsaturated pores would be equal to $(1 - S)$. Substituting Δz_p as S and Δz_f as $(1 - S)$ into eq. [25] gives

$$[26]\quad \frac{D^*(S)}{D^*(S=1)} = \frac{1}{\frac{S}{[1-\alpha S_r(1-S_e)/S]S} + \frac{(1-S)}{(1-S_e)\Re}}$$

The ratio of $(1 - S)$ to $(1 - S_e)$ in the second denominator term, which reduces to $(1 - S_r)$, is a constant. To reflect the contribution of the water films, the term $(1 - S)$ is arbitrarily raised to the power of 2. This is also consistent with the tortuosity factor given by Brooks and Corey (1966). The effect of degree of saturation on effective diffusion coefficient for case II is written as

$$[27]\quad \frac{D^*(S)}{D^*(S=1)} = \frac{1}{\frac{1}{[1-\alpha S_r(1-S_e)/S]} + \frac{(1-S)^2}{\Re(1-S_e)}}$$

Case III

In a more realistic framework, ions move simultaneously along the water-filled pores and water films interconnected in a series and parallel arrangement. The proportion of diffusion along the water-filled pores and the water films in a parallel and series arrangement can be represented by η and $(1 - \eta)$, respectively, and the normalized effective diffusion coefficient can be written as

$$[28] \quad \frac{D^*(S)}{D^*(S=1)} = \eta[\{1 - \alpha S_r(1 - S_e) / S\} S + \Re(1 - S_e)] + \frac{(1-\eta)}{\frac{1}{[1 - \alpha S_r(1 - S_e) / S]} + \frac{(1-S)^2}{\Re(1 - S_e)}}$$

Equations [17], [27], and [28] are the proposed mathematical models for predicting the relationship between the normalized effective diffusion coefficient and the degree of saturation, from S = 100% to $S = S_r$.

Laboratory test program

The primary objectives of the laboratory test program were to characterize the effect of the degree of saturation on the effective diffusion coefficient, and to verify the applicability of the theoretical models. The effective diffusion coefficient values at different matric suctions were defined on the basis of a single reservoir diffusion test for each value of matric suction. An olive brown, oxidized, uniform, fine to medium sand, Beaver Creek Sand (Bruch 1993), was selected for this study. A coarse-grained soil was chosen to simulate the drainage layer commonly present in a composite liner system and to understand the role of the liquid phase with regard to its interconnectivity with a decreasing degree of saturation. The physical, mineralogical, and chemical properties are provided in Table 2. Chloride and potassium ions were selected as the principal nonreactive and reactive tracers, respectively. One advantage of using potassium and chloride ions as chemical tracers is similarity in the diffusion coefficients in free water at 25°C ($D^o(K^+)$ = 1.96×10^{-9} m^2/s and $D^o(Cl^-)$ = 2.03×10^{-9} m^2/s) (Shackelford and Daniel 1991).

Diffusion tests were conducted at different matric suctions (i.e., at different water contents ranging from S = 100% to $S = S_r$). The program consisted of seven test setups at matric suctions of 0, 2.75, 2.95, 3.0, 3.6, 3.9, and 6.0 kPa. An independent, single reservoir diffusion test was also conducted on a 0.5 bar (1 bar = 100 kPa) high air entry disk in duplicate. The high air entry disk, which is located between the source reservoir and the soil specimen, formed an integral part of the single reservoir diffusion test for unsaturated soil. The coefficient of diffusion for the high air entry disk is, therefore, pertinent to determination of the effective diffusion coefficient for the soil.

For the reactive tracer (potassium), adsorption characteristics of the soil and high air entry disk were also defined on the basis of a 24 h batch-type test. Tests were performed in accordance with the American Society for Testing and Materials Standard D4646-87 (ASTM 1987) at various initial concentrations to define the shape of the adsorption function, m, and the adsorption coefficient, K_f, corresponding to S = 100%. The ratio of the dry mass of soil to the volume of potassium chloride solution was kept constant at one.

Table 2. Physical, mineralogical, and chemical properties of Beaver Creek Sand.

Soil property	Measured value
Grain-size distribution	
Percent sand	98.9
Percent passing U.S. No. 200 sieve	1.1
Coefficient of uniformity	1.8
Specific gravity	2.67
Mineralogy (%)	
Quartz	89.6
Plagioclase	8.71
Illite	1.24
Smectite	0.42
Fe–Mg chlorite	0.03
Cation exchange capacity (mequiv./100 g of dry soil)	1.3
Exchangeable cations (mequiv./100 g of dry soil)	
Ca^{2+}	0.86
Mg^{2+}	0.50
K^+	0.04
Na^+	0.06
Dissolved chemical species (mequiv./100 g of dry soil)	
Ca^{2+}	0.45
Mg^{2+}	0.20
K^+	0.02
Na^+	0.01
Cl^-	0.00
SO_4^{2-}	0.01
HCO_3^-	0.19

Single reservoir diffusion test

The apparatus for determining the effective diffusion coefficient of chloride and potassium for the sand and high air entry disks shown in Fig. 3 is described by Barbour et al. (1996). A brief description of the procedure for diffusion testing of soil is outlined here. The test setup and the test procedure for the high air entry disk are as described for the soil but without the soil specimen, porous stone, and loading cap.

Prior to the start of the test, the high air entry disk was flushed with at least 100 pore volumes of deaired, distilled, and deionized water (DDDW) to ensure complete saturation and chemical cleanliness. The source reservoir was then filled with DDDW followed by the placement of a magnetic stir bar into the reservoir and the high air entry disk. A known mass of air-dried soil was placed into a 79 mm diameter sample holder, and the cell was assembled with the porous stone, loading cap, and spring in place. A small preload equivalent to a pressure of 10 kPa was applied to the specimen to ensure continuity between the liquid phase in the soil and the high air entry disk. The mass of soil and the applied

Fig. 3. A single-reservoir diffusion cell used for determination of the effective diffusion coefficient for unsaturated soil.

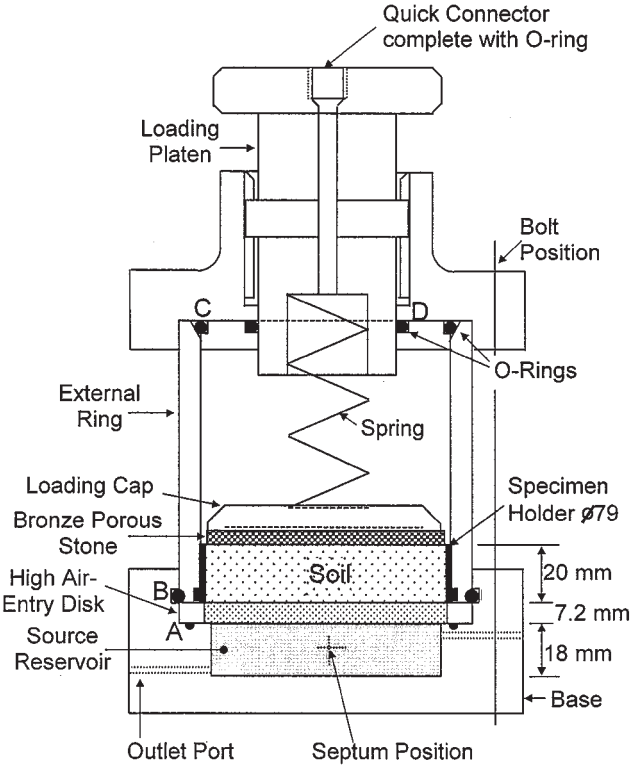

preload were maintained constant for all soil specimens to ensure uniformity in void ratio and dry density.

At the end of a 24 h equilibration period, the upper outlet was opened to allow excess water to drain under atmospheric conditions. An external air pressure was then introduced into the cell via the quick connector to drain the soil water to the desired matric suction using the axis translation technique (Hilf 1956). The external air pressure was regulated by means of a manometer. Once drainage was complete, the test was initiated by spiking the source reservoir with a volume of the stock solution (i.e., potassium chloride solution). A sample of less than 1 mL was then taken immediately from the source reservoir to establish the initial concentration. The initial concentrations of potassium and chloride in the source reservoir ranged from 0.02 to 0.023 M.

Changes in the reservoir concentrations were monitored at various time intervals by sampling the reservoir solution. To ensure a uniform concentration within the reservoir during sampling, the reservoir solution was gently stirred for approximately 2 min. The test was terminated when changes in the reservoir concentration were insignificant (i.e., the solute concentration is in equilibrium or uniform throughout the entire system). Upon completion of the diffusion test, the soil specimen was extruded and sliced into smaller segments for water content and chemical mass balance determinations. The water contents of the soil segments were measured by drying the soil at a room temperature of 21.2°C instead of oven drying to avoid changes to the soil chemistry due to the temperature effect. The small difference in water content between oven-dried and air-dried soil samples of 0.1% was deemed to be insignificant to interpretation of the results.

Data analysis

Back-analysis for the coefficient of diffusion coefficient was dependent upon the interactions between the tracers and the soil. For the nonreactive tracer (chloride), the required effective diffusion coefficient was determined by fitting various predictions of the decrease in the reservoir concentration with time to the measured concentration versus time profile. The theoretical concentration versus time profiles were simulated using the CTRAN/W program, and the required effective diffusion coefficient was obtained by varying the diffusion coefficient until an acceptable fit between the measured and predicted profiles was obtained. CTRAN/W is proprietary computer software based on a finite element formulation (Geo-Slope International Ltd. 1991).

The CTRAN/W program was formulated for a two-dimensional contaminant-transport problem. For simplicity, the governing differential equation derived from the continuity equation shown here is for one-dimensional contaminant transport of a reactive solute:

$$\underset{\text{rate of mass change}}{\left(\theta_w + \rho_d \frac{\partial Q_{ad}}{\partial C}\right)\frac{\partial C}{\partial t}} \quad \underset{\text{diffusion term}}{= \theta_w D \frac{\partial^2 C}{\partial x^2}} \quad \underset{\text{advection term}}{- \theta_w v \frac{\partial C}{\partial x}} \quad \underset{\text{adsorption term}}{- \rho_d Q_{ad}} \qquad [29]$$

where

θ_w is the volumetric water content;
ρ_d is the dry density of soil;
Q_{ad} is the mass of solute adsorbed by soil per unit mass of dry soil;
C is the solute concentration;
t is the elapsed time;
D is the dispersion coefficient and is equal to ($\alpha v + D^*$), where α is the dispersivity and D^* is the effective diffusion coefficient;
v is the linear velocity or seepage velocity; and
x is the macroscopic length of an elemental volume in the x direction.

For unsaturated soil, the terms K_f associated with Q_{ad}, D^*, and v are functions of degrees of saturation. The Galerkin equation was used to derive the finite element equation using a general set of interpolating functions presented by Bathe (1982). Time integration can be performed using either a backward-difference or a central-difference approximation; both methods were incorporated within CTRAN/W. The finite element model for the test, including the boundary conditions, is shown in Fig. 4. The test setup was idealized as a column consisting of eight-noded higher order quadrilateral elements with different material properties representing the source reservoir, high air entry disk, soil specimen, and porous stone. For the initial condition ($t = 0$), the nodes of the reservoir elements were set equal to the initial con-

Fig. 4. Idealization of the diffusion test setup for back-calculation of the effective diffusion coefficient using the CTRAN/W program. Volumetric water content θ_w is 0.53 for the high air entry disk and 0.05 for the porous stone. C_b, background concentration; C_o, initial reservoir concentration; N, number of elements.

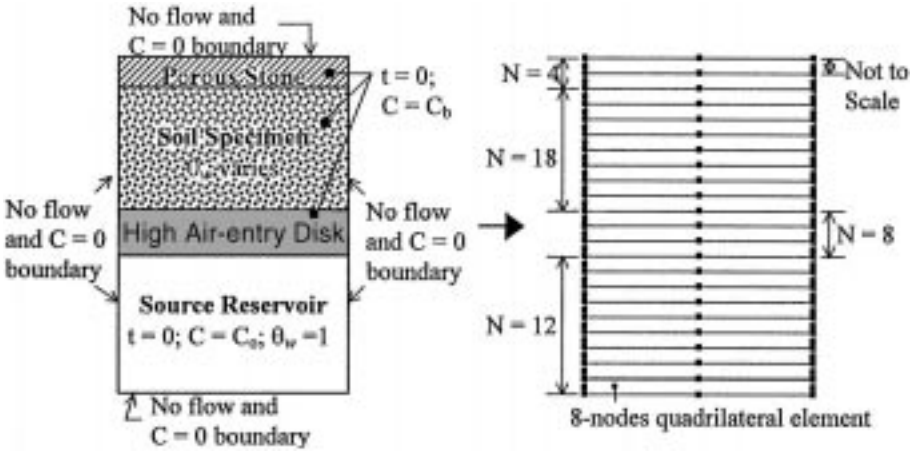

centration, C_o. A value equal to the measured background concentration, C_b, was assigned to the remaining nodes. Simulation of the diffusion test was divided into a number of time increments; each increment corresponds to the actual sampling time. Preliminary validation of the program was made by comparing the analysis against the results obtained from POLLUTE (Rowe and Booker 1983) using fictitious examples at various degrees of saturation (i.e., volumetric water contents) for cases of nonreactive and reactive solutes. Trial runs were carried out to optimize the element size and the size of the time step for each time increment to obtain a more accurate solution.

In the case of the reactive tracer (potassium), changes in the reservoir concentration with time were related to both diffusion and adsorption processes. The back-analysis for the unknown coefficients of diffusion and adsorption was different for cases in which chemical equilibrium was attained at the end of the test and those cases with incomplete chemical equilibrium.

For cases in which chemical equilibrium was attained at the end of the test, the pore-water concentration of the high air entry disk and the soil was uniform and equal to the final reservoir concentration. The adsorption coefficient, $K_f(S)$, for the soil can be obtained using Freundlich's equation given in eq. [6] with m defined by the 24 h batch-type test (Standard D4646-87, ASTM 1987), and the mass adsorbed by the soil per unit mass of dry soil, Q_{ad}, is given as

$$[30] \quad Q_{ad} = \frac{M_{tot} - C_f V_w}{M_s}$$

where

M_{tot} is the total mass of potassium in the soil specimen at the end of a diffusion test;
C_f is the final reservoir concentration;
V_w is the volume of soil water; and
M_s is the mass of air-dry soil.

The total mass of potassium in the soil specimen at the end of the diffusion test, M_{tot}, was extracted by saturating the air-dried soil in DDDW followed by four additional extractions in 0.1 N barium chloride solution using the principle of ion exchange. The duration of each extraction was more than 24 h. At the end of each extraction step, the supernatant was decanted before adding a fresh saturating solution. The remaining unknown coefficient of diffusion was determined as described for nonreactive tracer.

For cases in which chemical equilibrium was not attained at the end of a diffusion test, the coefficients of diffusion and adsorption were unknown. The unknown coefficients were back-calculated by matching the reservoir concentration versus time profile, and the potassium concentration(s) in the soil water simultaneously using CTRAN/W. A solution was obtained when both the simulated concentration versus time and concentration versus depth profiles matched the respective measured profiles. The potassium concentration of the soil water was calculated by trial and error, based on the total mass extracted from the soil, M_{tot}, and the adsorption coefficient assumed in the numerical simulation:

$$[31] \quad M_{tot} = C_{sw}V_{sw} + K_f(S)(C_{sw})^m M_s$$

where

C_{sw} is the concentration of potassium in soil water;
V_{sw} is the volume of soil water; and
M_s is the mass of dry soil.

Various combinations of different values of the effective diffusion and adsorption coefficients were evaluated systematically by either varying the effective diffusion coefficient while keeping the adsorption coefficient constant, or vice versa.

A mass-balance check was also evaluated for the various ions. For chloride, mass conservation was made based on the difference between initial and final mass:

$$[32] \quad \sum M = \{C_o V_r + C_b V_{dss}\}_{\text{initial}} - M_{sa} - C_f V_t$$

where

Fig. 5. Measured and simulated reservoir concentration of chloride and potassium versus time profiles for 0.5 bar high air entry disks.

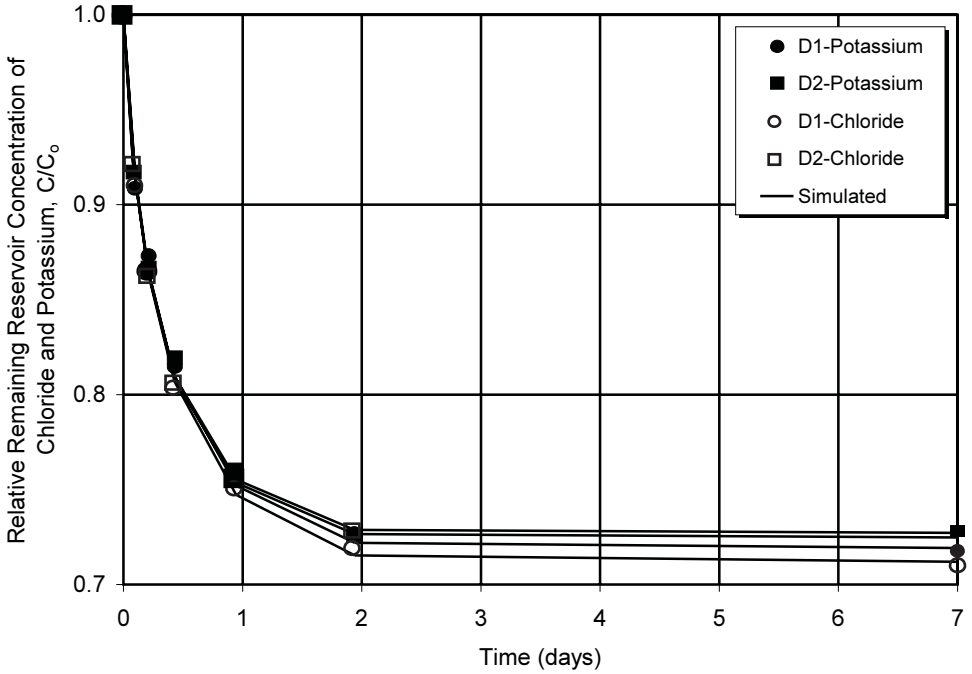

Table 3. Back-calculated effective diffusion coefficients of chloride and potassium for the 0.5 bar high air entry disks.

Disk No.	Chemical species	Effective diffusion coefficient ($\times 10^{-9}$ m^2/s)	Apparent adsorption coefficient (mL/g)
D1	K^+	0.75	0.086
	Cl^-	0.75	0.100
D2	K^+	0.70	0.080
	Cl^-	0.75	0.065

$\sum M$ is the mass balance of tracer at the end of the diffusion test;
C_o is the initial reservoir concentration;
V_r is the volume of water in the source reservoir;
C_b is the background concentration in high air entry disk, soil, and porous stone at the start of the diffusion test;
V_{dss} is the volume of water in the pores of the high air entry disk, soil, and porous stone;
M_{sa} is the mass of tracer removed during sampling for chemical analysis;
C_f is the final concentration in the reservoir; and
V_t is the total volume of water in the diffusion cell (i.e., volume in the reservoir and pores of the high air entry disk, soil, and porous stone).

The mass conservation of potassium was evaluated by comparing the total mass extracted from the soil specimen against the theoretical value. The theoretical mass was calculated based on the difference between the initial mass in the system and the final mass in the reservoir, high air entry disk, and porous stone:

$$[33] \quad \sum M = M_{tot} - \{(C_o V_r + C_b V_{dss}) - (C_f V_t + M_{sa} + M_{add})\}$$

where M_{add} is the mass adsorbed by the high air entry disk.

For the high air entry disks, the diffusion tests were run for at least 7 days and were terminated only when changes in the reservoir concentration were insignificant, which suggested that a uniform concentration was established throughout the liquid phase. Any imbalance in mass at the end of the diffusion test was ascribed to that adsorbed by the disk. The remaining unknown effective diffusion coefficient was determined as it was for the soil and the adsorption characteristic was also described by Freundlich's equation with m set equal to one.

Results

High air entry disks

The decreases in concentration of potassium and chloride in the source reservoir with time for the 0.5 bar high air entry disks are shown in Fig. 5 along with the simulated concentration versus time profiles that best matched the measured data. Results showed that changes in the reservoir concentrations were practically insignificant after 2 days. The tests, which were terminated after an elapsed time of 7 days, would have attained complete chemical equilibrium at the end of the tests. The back-calculated effective diffusion coefficients of chloride and potassium and the respective ad-

Fig. 6. Adsorption characteristics of the sand and 0.5 bar high air entry disk for potassium defined on the basis of a 24 h batch-type test in accordance with ASTM Standard D4646-87 (ASTM 1987).

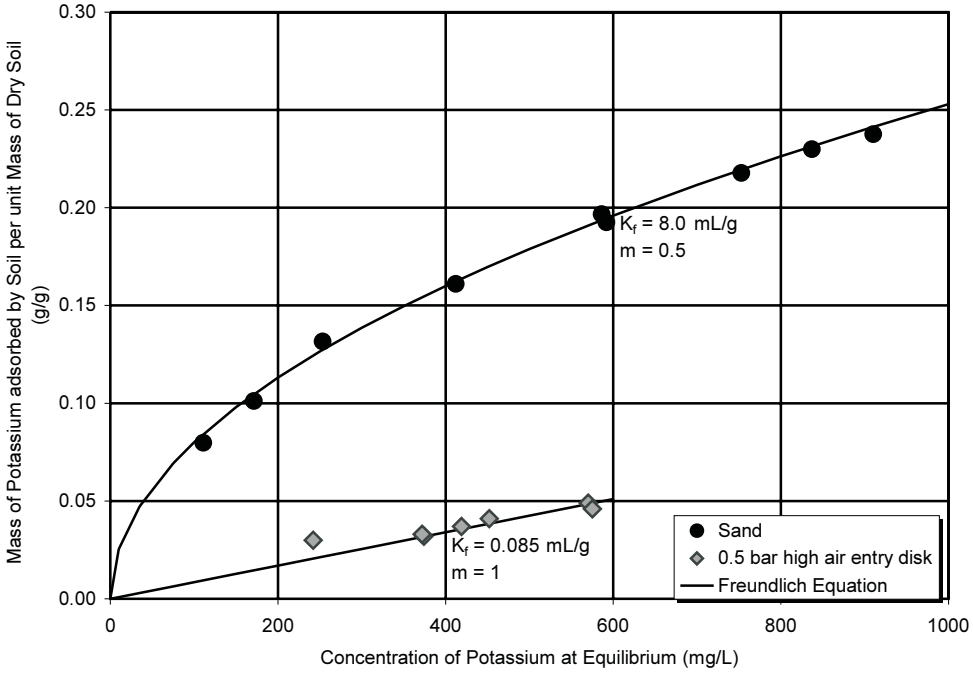

Fig. 7. Variation of the degree of saturation across the soil profile for sand at different matric suctions.

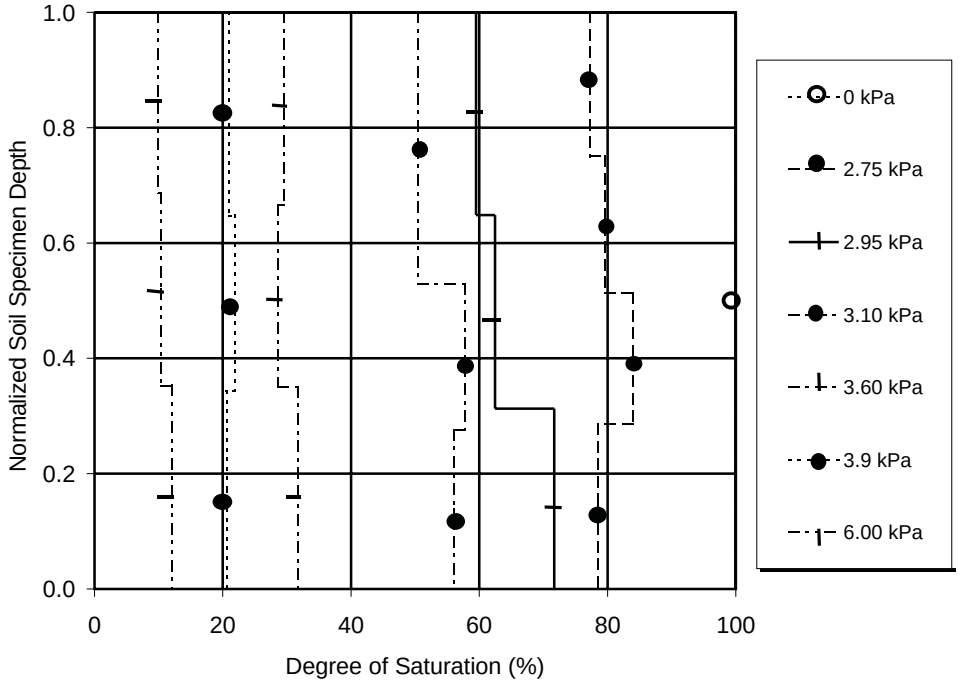

sorption coefficients representing the mass loss are summarized in Table 3. The adsorption characteristic of the disk for potassium defined on the basis of a 24 h batch-type test is given in Fig. 6.

Beaver Creek Sand

The physical index properties of the soil specimens for the different cases of matric suction were calculated based on the water content and the total volume of the soil specimen at the end of a diffusion test. The porosity and dry density of the soil specimens were 38.2 ± 0.3% and 1647 ± 7 kg/m^3, respectively. Variations of the degree of saturation across the soil profile and the relationship between the degree of saturation and the suction for the different cases of matric suction are shown in Figs. 7 and 8, respectively. A S_r value of 9% was estimated using a method described by Brooks and Corey (1966).

The adsorption characteristic of the sand for potassium defined by a 24 h batch-type test is shown in Fig. 6. Variations of the concentrations of chloride and potassium in the

Fig. 8. Relationship between the degree of saturation and suction for sand at different matric suctions.

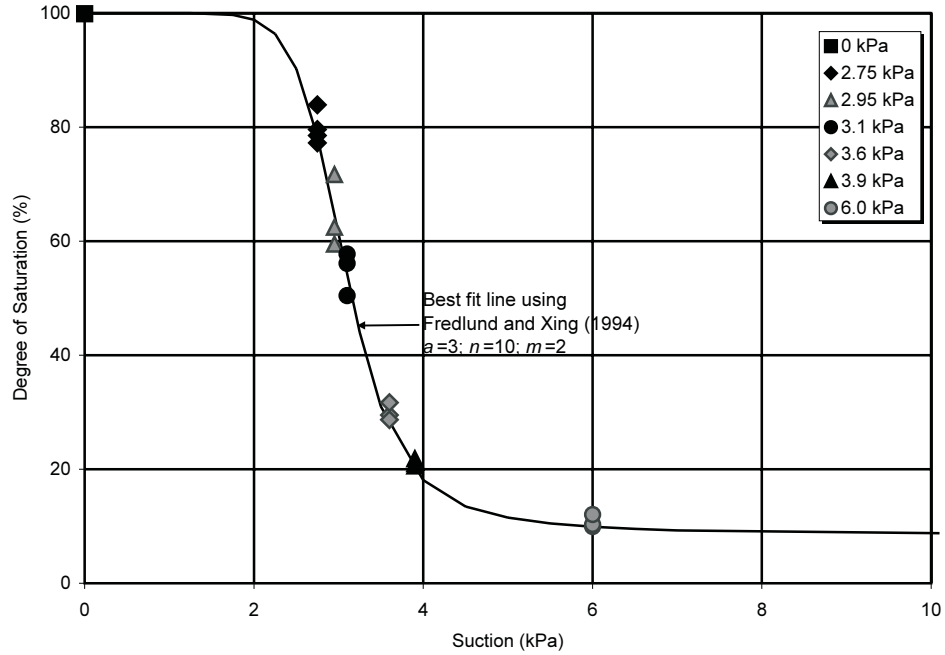

Fig. 9. Measured reservoir concentration of chloride versus time profiles for sand at different matric suctions and the simulated profiles for selected cases.

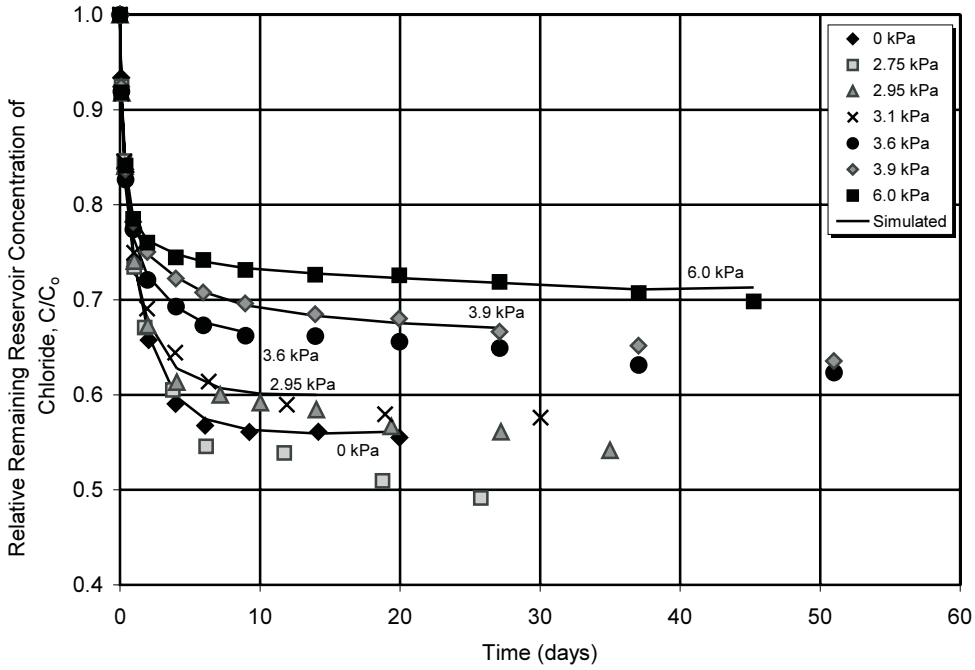

source reservoir with time for cases at different matric suctions are given in Figs. 9 and 10. The results showed that, in general, the concentration versus time profiles were characterized by a smooth decreasing trend. The similarity in the profiles during the initial stages of the tests was due to diffusion through the high air entry disk.

The general shape of the concentration versus time profile for chloride showed that the concentrations for different matric suctions "level off" much earlier than for potassium. The final concentration of chloride was also consistently higher than that for potassium for corresponding matric suctions. The results also showed that the rate of change of the reservoir concentration of potassium and chloride decreased with an increase in matric suction in the soil (i.e., a decrease in the degree of saturation). The slower equilibrium time and the lower final concentration for potassium were likely due to the adsorption-exchange reactions.

Conservation of mass for the various ions was checked and a summary of the results for chloride and potassium are provided in Tables 4 and 5, respectively. For chloride, the results showed a significant difference between the initial and final mass ranging from 0.8 to 17.3%. The mass loss

Fig. 10. Measured and simulated reservoir concentration of potassium versus time profiles for sand at different matric suctions.

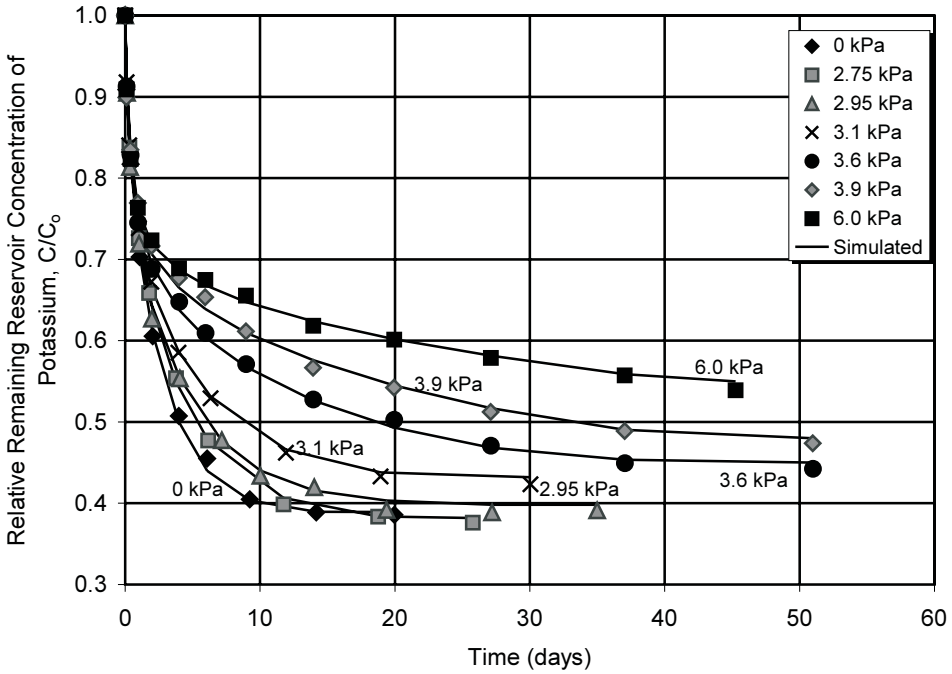

Table 4. Measured and theoretical total mass of chloride at the end of the test for sand at different matric suctions.

Matric suction (kPa)	Measured total mass (mg, ±SE)	Theoretical total mass (mg)	Percent difference (±SE)[a]
0	55.0 ± 0.6	57.36	4.0 ± 1.0
2.75	49.8 ± 0.5	60.30	17.3 ± 0.9
2.95	54.6 ± 0.6	62.01	12.0 ± 1.0
3.1	55.1 ± 0.6	60.87	9.5 ± 1.0
3.6	57.4 ± 0.7	61.73	7.0 ± 1.1
3.9	56.3 ± 0.7	60.93	7.6 ± 1.2
6.1	58.8 ± 0.8	59.24	0.8 ± 1.3

[a] Calculated as (theoretical – measured)/theoretical × 100%.

Table 5. Measured and theoretical mass of potassium in the soil specimen at the end of the test for sand at different matric suctions.

Matric suction (kPa)	Measured total mass (mg, ±SE)	Theoretical total mass (mg)	Percent difference (±SE)[a]
0	29.3 ± 0.3	33.1	11.6 ± 1.0
2.75	28.6 ± 0.1	29.8	3.8 ± 0.4
2.95	28.4 ± 0.1	29.5	3.7 ± 0.3
3.1	25.0 ± 0.2	26.3	4.7 ± 0.7
3.6	22.7 ± 0.1	24.0	5.1 ± 0.5
3.9	20.7 ± 0.1	21.3	2.3 ± 0.2
6.2	14.9 ± 0.1	15.1	0.8 ± 0.7

[a]Calculated as (theoretical – measured)/theoretical × 100%.

may be due to possible chemical reactions between chloride and the bronze coating on the porous stone. Chloride is known to react with aluminum, and the same reaction may be operative, particularly with new bronze porous stone. The color on the porous stone changed from bright golden to dull brown by the end of the test. In the case of potassium, the results showed a difference of less than or equal to 5% between the measured and the theoretical total mass in the soil specimen for all cases, except for the case of matric suction of 0 kPa.

The simulated concentration versus time profiles for the reservoir which best match the measured data for chloride

Fig. 11. Simulated soil-water concentrations of potassium across the soil profile and measured concentrations for the sand at different matric suctions.

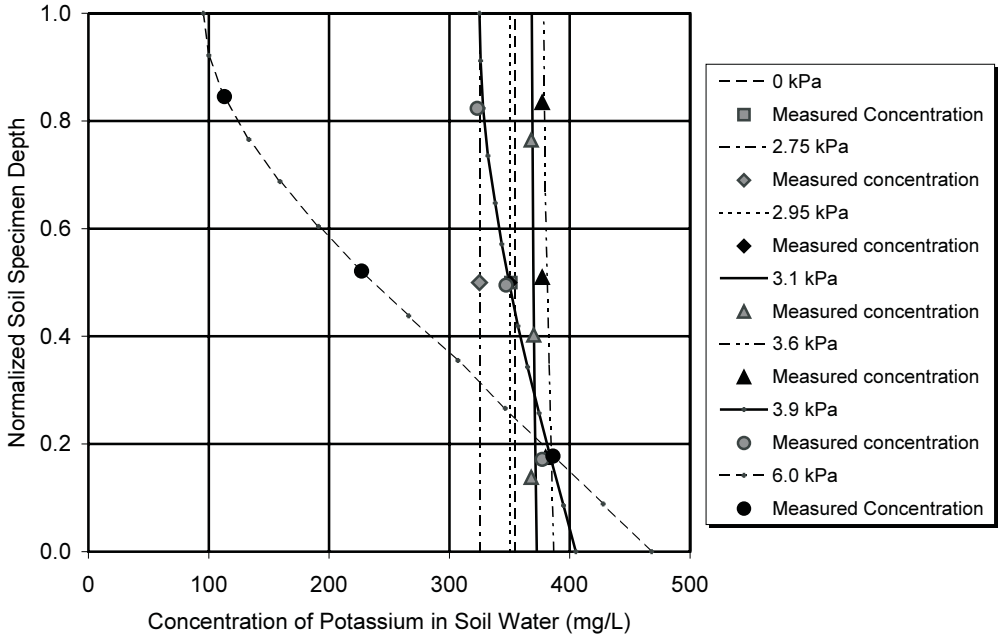

Table 6. Back-calculated effective diffusion coefficients of chloride and potassium for the sand at different matric suctions.

		Chloride		Potassium		
Matric suction (kPa)	Degree of saturation (%)	$D^*(S)(\times 10^{-9}\,m^2/s)$	$\frac{D^*(S)}{D^*(S=1)}$	$D^*(S)(\times 10^{-9}\,m^2/s)$	$\frac{D^*(S)}{D^*(S=1)}$	$K_f(S)$ (L/mg)
0	~100	1.40	1.00	1.20	1.00	10.00
2.75	~80	—	—	0.7–0.8	0.58–0.67	9.75
2.95	~65	1.00	0.71	0.70	0.58	9.50
3.1	~53	—	—	0.60	0.50	8.33
3.6	~30	0.80	0.57	0.40	0.33	8.26
3.9	21	0.50	0.36	0.30	0.25	8.20
6.0	~10	0.40	0.28	0.225	0.19	6.70

and potassium are plotted in Figs. 9 and 10. For chloride, only cases with mass-balance errors of less than 10% were evaluated. The best fit between the measured and simulated profiles was selected by minimizing the differences between the predicted and measured concentrations among the various simulations. The simulated concentration versus depth profiles for potassium in the soil water and the soil water concentrations calculated using eq. [31] are given in Fig. 11. A summary of the back-calculated effective diffusion coefficients of chloride and potassium for the different values of matric suction, including the absorption coefficient of potassium, are given in Table 6.

The match between the simulated and the measured concentration versus time profiles for the various cases of matric suction, in general, was very satisfactory for both chloride and potassium. The level of agreement between the potassium concentrations of the soil water and the simulated concentration versus depth profile for different matric suctions was also reasonably good. For matric suctions of 0, 2.75, 2.95, and 3.1 kPa, the simulated concentration versus depth profiles were uniform and this may further suggest that chemical equilibrium was indeed attained at the end of the diffusion test.

Effect of the degree of saturation on the coefficient of diffusion

Results of the effective diffusion coefficients of chloride and potassium, normalized with respect to the effective diffusion coefficient corresponding to S = 100%, versus the degree of saturation are given in Fig. 12. The effective diffusion coefficient at S = 100% was based on the coefficient corresponding to the case with a matric suction of 0 kPa (i.e., a degree of saturation of 99.9%).

The results for chloride were quite scattered. Values of the normalized diffusion coefficients corresponding to matric suctions of 2.95 and 3.6 kPa were much higher than those for potassium. The general trend showed a decrease in the normalized diffusion coefficient with a decrease in degree of saturation, although a further verification of the form of the functional relation is needed. The results for potassium showed a definite trend of a decrease in the normalized dif-

Fig. 12. Results of the back-calculated effective diffusion coefficients of potassium and chloride, normalized with respect to the effective diffusion coefficient at S = 100%, versus degree of saturation for the sand.

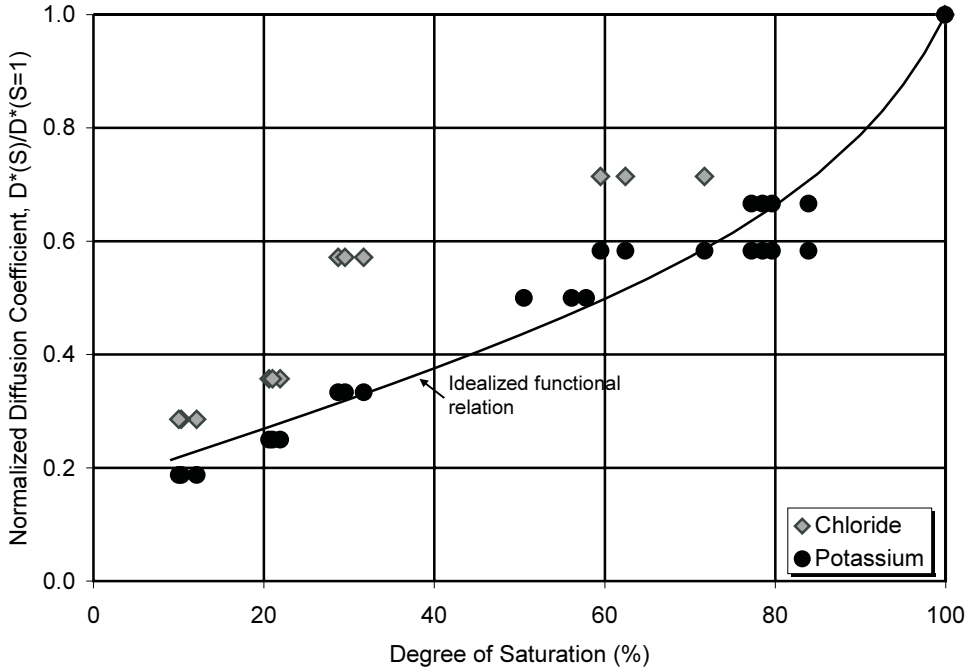

Fig. 13. Results of the back-calculated normalized diffusion coefficient of potassium at various degrees of saturation for sand and the predicted values calculated based on case I, eq. [17] (i.e., diffusion in a parallel arrangement).

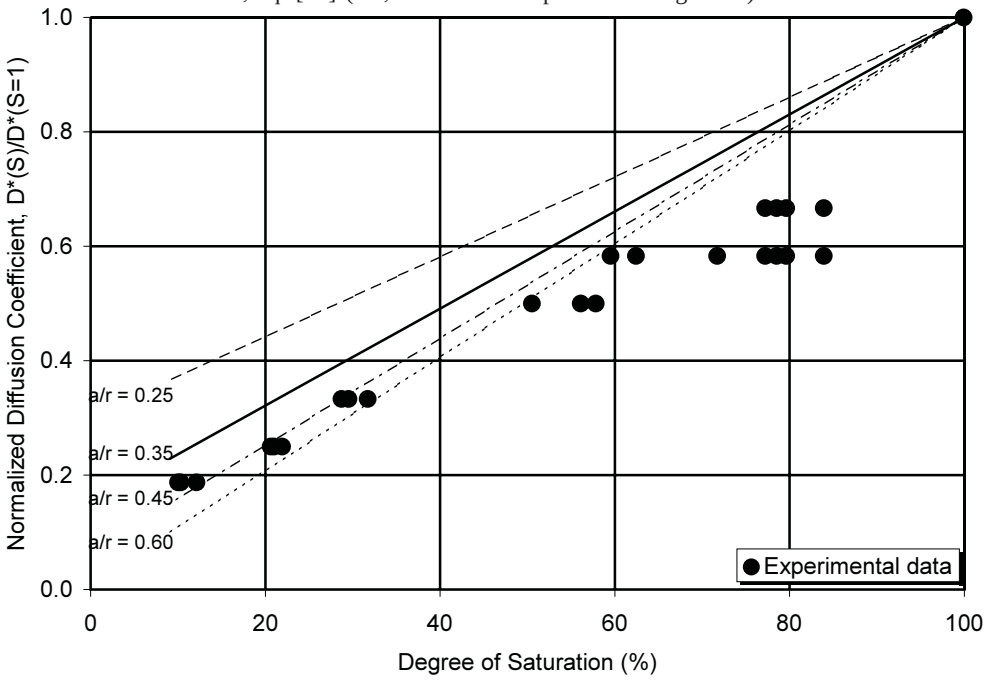

fusion coefficient with decreasing degree of saturation. The normalized diffusion coefficient decreased from 1.0 at S = 100% to 0.19 as the degree of saturation approached S_r. The idealized functional relation for the normalized diffusion coefficient of potassium was slightly nonlinear.

Model verification

The applicability of the theoretical models given in eqs. [17], [27], and [28] were evaluated for cases with parallel, series, and combined arrangements, respectively, in predicting the coefficient of diffusion for the sand. Verification of the models was based on the back-calculated normalized diffusion coefficient of potassium only. The various predictions were calculated by setting the a/r ratio (i.e., the ratio of the radius of the hydrated ion to the radius of the pore) as the parameter variable. The other parameters required for the models were the residual degree of saturation and the fraction of the water content contained in water films near the residual degree of saturation, α. The residual degree of saturation for the sand was 9%. The factor, α, calculated based

Fig. 14. Results of the back-calculated normalized diffusion coefficient of potassium at various degrees of saturation for sand and the predicted values calculated based on case II, eq. [27] (i.e., diffusion in a series arrangement).

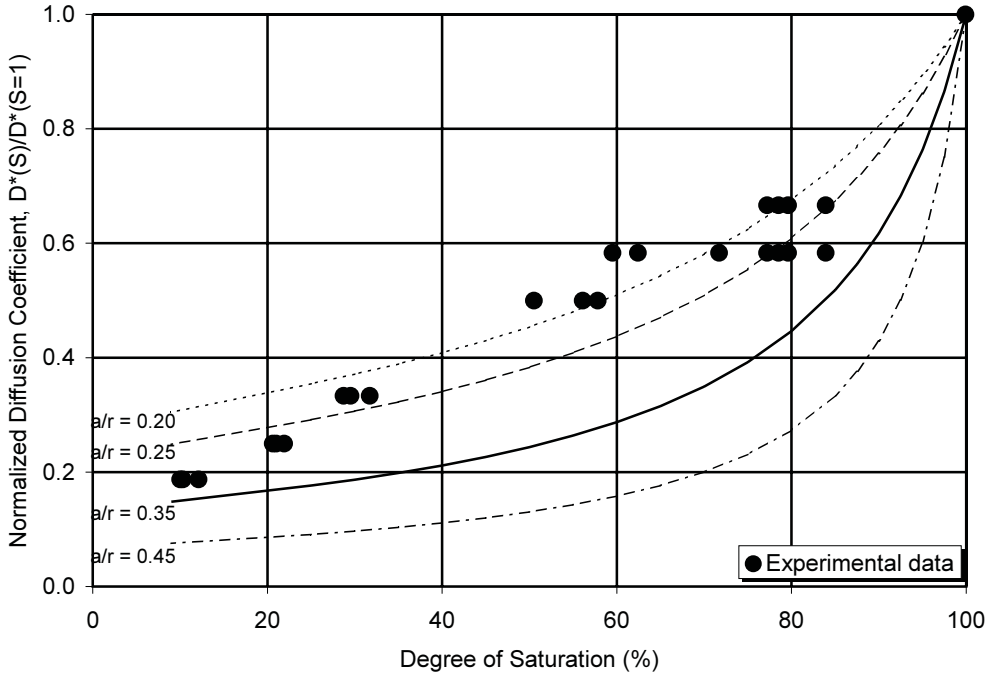

Fig. 15. Results of the back-calculated normalized diffusion coefficient of potassium at various degrees of saturation for sand and the predicted values calculated based on case III, eq. [28] (i.e., combination of cases I and II).

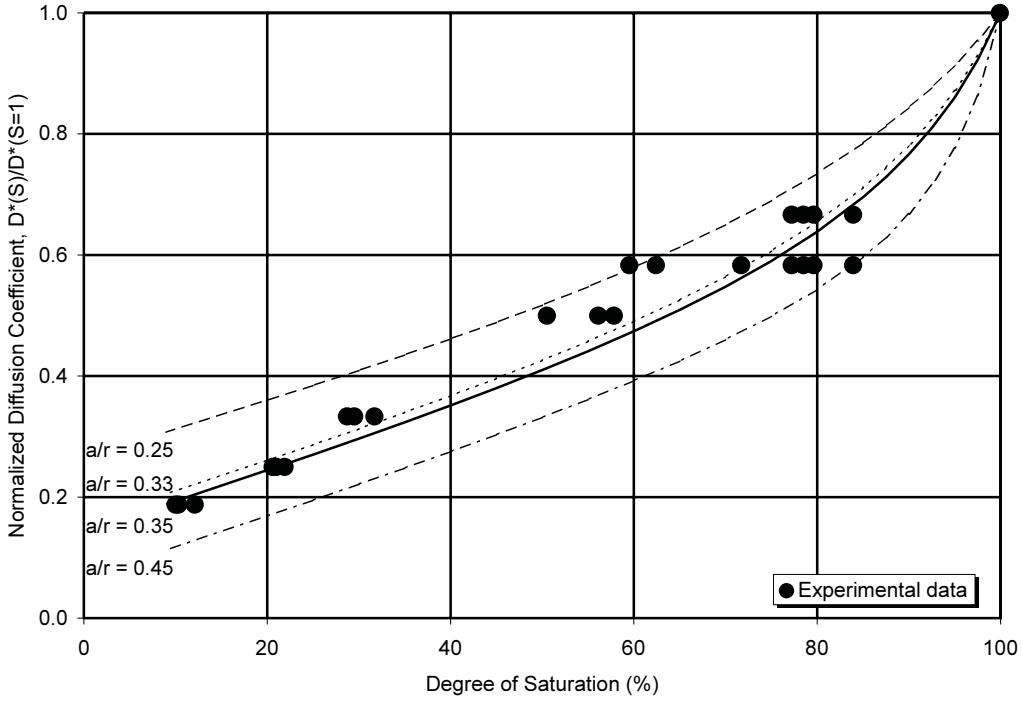

on the total surface area of the soil and an assumed water film thickness of three molecular layers of water (i.e., 1 nm) was rounded off to 0.1 to include the isolated water in the pore throats.

The predicted functional relationships corresponding to various a/r ratios for the parallel, series, and combined models and the back-calculated normalized diffusion coefficient of potassium are given in Figs. 13–15. For the combined model, the η value was set equal to 0.5, assuming that the probability of the ions diffusing along the various pathways in either a parallel or a series arrangement is equal. The results showed that the functional form of eq. [17] describing

diffusion along independent water-filled pores and water films in a parallel arrangement is linear, whereas those of eqs. [27] and [28] for the series and combined models are nonlinear.

The results also showed that the match between the back-calculated normalized diffusion coefficients and the predicted linear function of the parallel model (i.e., case I) was unsatisfactory, regardless of the a/r ratios. Between the series (i.e., case II) and the combined (i.e., case III) models, the functional form corresponding to an an a/r ratio of 0.33 of the combined model provided a more satisfactory match of the experimental data. The thickness of the water film corresponding to an a/r ratio of 0.33 calculated based on a hydrated diameter of 0.33 nm (Horvath 1985) was also 1.0 nm, which is the same as that used in calculating α.

The model verification based on a rather limited set of data for a sand showed that the nonlinear functional form based on the series and combined models could provide a reasonably good prediction of the effective diffusion coefficient at various degrees of saturation. The prediction, however, is dependent on the a/r ratio.

Conclusions

Theoretical models for the prediction of the effective diffusion coefficient for unsaturated soils were developed. Three diffusion modes were considered: case I, in which diffusion is assumed to occur independently along continuous water-filled pores and water films in a parallel arrangement; case II, in which diffusion is assumed to occur along interconnected water-filled pores and water films in a series arrangement; and case III, in which diffusion is assumed to occur in an arrangement combining those of cases I and II.

Diffusion tests were conducted on a sand at different matric suctions (i.e., different water contents ranging from 100% to the residual degrees of saturation) to characterize the effective coefficient as a function of degrees of saturation and to verify the applicability of the models. Chloride and potassium ions were used as the principal nonreactive and reactive tracers.

Mass balance of the tracers at the end of the test was evaluated for the different matric suctions. The mass-balance check showed a significant difference between the initial and final mass of chloride ranging from 10 to 18%. For potassium, the percent difference between the actual and theoretical mass in the soil specimen for most cases was less than 5% except for the matric suction of 0 kPa.

Results of the back-calculated effective diffusion coefficient of chloride and potassium at various degrees of saturation, in general, showed a decrease in the coefficient with a decrease in degree of saturation. For chloride, the results were quite scattered and a further verification of the form of the functional relation is needed. For potassium, the results showed a definite trend of a decrease in the normalized diffusion coefficient with decreasing degree of saturation. The normalized diffusion coefficient decreased from 1.0 at S = 100% to 0.19 as the degree of saturation approached S_r. The idealized functional relation for the normalized diffusion coefficient of potassium was slightly nonlinear.

Results from the model verification showed that the functional form of eq. [17] describing diffusion along independent water-filled pores and water films in a parallel arrangement is linear, whereas eqs. [27] and [28] for the series and combined models, respectively, are nonlinear. The match between the back-calculated normalized diffusion coefficients and the predicted linear function of the parallel model (i.e., case I) is unsatisfactory, regardless of the a/r ratios. Between the series and the combined models, the functional form corresponding to an an a/r ratio of 0.33 of the combined model seemed to give a more satisfactory match of the experimental data.

Model verifications based on a rather limited set of data for a sand showed that the nonlinear functional form based on the model which combines the series and parallel arrangements can provide a reasonably good prediction of the effective diffusion coefficient at various degrees of saturation. The prediction, however, is dependent on the a/r ratio.

References

Allison, J.M., and Bergman, T.B. 1988. The Hanford Grout Treatment Facility — environmental assurance in low level waste disposal. *In* Spectrum 88, Proceedings of the International Topical Meeting on Nuclear and Hazardous Waste Management, Pasco, Wash., pp. 130–132.

ASTM. 1987. Standard test method for 24-hour batch-type measurement of contaminant sorption by soils and sediments (D4646-87). *In* 1987 Annual Book of ASTM Standards. American Society for Testing and Materials, Philadelphia, Pa., pp. 122–125.

Barbour, S.L., Lim, P.C., and Fredlund, D.G. 1996. A new technique for diffusion testing of unsaturated soil. Geotechnical Testing Journal, ASTM, **19**(3): 247–258.

Barraclough, P.B., and Tinker, P.B. 1981. The determination of ionic diffusion coefficients in field soils I. Diffusion coefficients in sieved soils in relation to water content and bulk density. Journal of Soil Science, **32**: 225–236.

Bathe, K.J. 1982. Finite element procedures in engineering analysis. Prentice-Hall, Inc., Englewood Cliffs, N.J.

Brooks, R.H., and Corey, A.T., 1966. Properties of porous media affecting fluid flow. Journal of the Irrigation and Drainage Division, ASCE, **92**(IR2): 61–88.

Bruch, P. 1993. Evaporative fluxes in homogenous and layered soils. M.Sc. thesis, Department of Civil Engineering, University of Saskatchewan, Saskatoon, Sask.

Conca, J.L., and Wright, J. 1990. Diffusion coefficients in gravel under unsaturated conditions. Water Resources Research, **26**(5): 1055–1066.

Fredlund, D.G., and Xing, A. 1994. Equations for the soil-water characteristic curve. Canadian Geotechnical Journal, **31**: 521–532.

Geo-Slope International Ltd. 1991. CTRAN/W users manual, version 2. Geo-Slope International Ltd., Calgary, Alta.

Hilf, J.W. 1956. An investigation of pore-water pressure in compacted cohesive soils. Ph.D. thesis, Technical Memorandum No. 654, U.S. Department of the Interior, Bureau of Reclamation, Design and Construction Division, Denver, Colo.

Hillel, D. 1980. Fundamentals of soil physics. Academic Press, New York.

Horvarth, A.L. 1985. Handbook of aqueous electrolyte solutions — physical properties, estimation and correlation methods. Ellis Horwood Limited, Chichester, U.K.

Klute, A., and Letey, J. 1958. The dependence of ionic diffusion on the moisture content of non-adsorbing porous media. Soil Science Society of America Proceedings, **22**: 213–215.

Olsen, S.R., and Kemper, W.E. 1968. Movement of nutrients to plant roots. Advances in Agronomy, **20**: 91–151.

Porter, L.K., Kemper, W.D., Jackson, R.D., and Stewart, B.A. 1960. Chloride diffusion in soils as influenced by moisture content. Soil Science Society of America Proceedings, **24**: 460–463.

Renkin, E.M. 1955. Filtration, diffusion, and molecular sieving through porous cellulose membranes. Journal of General Physiology, **38**: 225–243.

Robinson, R.A., and Stokes, R.H. 1959. Electrolyte solutions. 2nd ed. Butterworths, London.

Romkens, M.J.M., and Bruce, R.R. 1964. Nitrate diffusivity in relation to moisture content of non-adsorbing porous media. Soil Science, **98**: 332–337.

Rowe, R.K., and Booker, J.R. 1983. Program POLLUTE — 1Q pollutant migration analysis program. Geotechnical Research Center, Faculty of Engineering Science, The University of Western Ontario, London, Ont.

Rowell, D.L., Martin, M.W., and Nye, P.H. 1967. The measurement and mechanism of ion diffusion in soils. III. The effect of moisture content and soil solution concentration on the self diffusion of ions in soils. Journal of Soil Science, **18**: 204–222.

Shackleford, C.D., and Daniel, D.E. 1991. Diffusion in saturated soils: I. Background. Journal of Geotechnical Engineering, ASCE, **117**(3): 467–484.

van Rees, K.C.J. 1989. Predicting potassium uptake for *Pinus elliottii* Engelm. var. *elliottii* using diffusion/mass-flow nutrient supply theory. Ph.D. dissertation, University of Florida, Gainesville, Fla.

Warncke, D.D., and Barber, S.A. 1972. Diffusion of zinc in soil: I. The influence of soil moisture. Soil Science Society of America Proceedings, **36**: 39–42.